CONSTITUTIVE MODELS AND STRAIN LOCALIZATION IN POROUS SANDSTONE

K.A. Issen and V. Challa
Department of Mechanical and Aeronautical Engineering, Clarkson University, Potsdam, NY 13699 USA

ABSTRACT

Field and laboratory observations find that porous sandstone often fails via bands of localized strain that consist of shear deformation and/or deformation normal to the band. Of particular interest are the recently observed compaction bands, which consist of pure compressional deformation (no shear offset). Conditions for compaction band formation, determined using the localization theory of Rudnicki and Rice (1975), depend on constitutive model details. The three existing constitutive models examined here employ either one or two yield surfaces, each paired with a corresponding plastic potential. A proposed new model uses a single yield surface with two plastic potentials, representing the two microstructural damage processes observed in high porosity sandstone (dilatant microcracking and compactive grain crushing with pore collapse). A damage characterization parameter, representing the ratio of the magnitudes of the inelastic strains due to the two damage processes, is utilized to establish a stress region where both process are active, corresponding to the observed brittle – ductile transitional regime where compaction bands are observed. For overall compactive behavior (dilation coefficient and yield surface slope are both negative), the single yield surface models, including the proposed model, produce the same compaction band condition, which is not satisfied by experimentally reported data for compaction band formation. Thus, the additional flexibility provided by adding a second plastic potential to a single yield surface model does not alter the constitutive framework enough to change the localization conditions. However, the addition of a second yield surface corresponding to the second plastic potential does significantly alter both the constitutive framework and the localization conditions, such that the observed compaction bands are predicted.

1 INTRODUCTION

Strain localization, in the form of planar bands consisting of shear deformation, often accompanied by either dilatant or compactant deformation normal to the band, is a commonly observed failure mode in porous sandstone. Recently, bands consisting of pure compaction (no shear), have been observed in field and laboratory settings. Mollema and Antonellini (1996) described compaction bands in aeolian Navajo sandstone (20-25% porosity) as thin tabular zones of pure compressional deformation, with no shear offset, that formed perpendicular to the direction of maximum compression. Compaction bands and/or shear bands were observed in laboratory axisymmetric compression (ASC) tests by Olsson (1999) on Castlegate sandstone (28% porosity), and by Wong et al. (2001) in Bentheim, Berea and Darley Dale sandstones (porosities of 23%, 21% and 13%, respectively).

The strain localization theory of Rudnicki and Rice (1975) was originally developed to predict the onset of shear localization in dilatant low porosity rock. However, Olsson (1999) suggested that the same theoretical framework could be used to predict formation of the compaction bands he observed in high porosity sandstone. Issen and Rudnicki (2000, 2001) subsequently reexamined the work of Rudnicki and Rice (1975) and identified the localization conditions for compaction

bands. Previously, Ottosen and Runesson (1991) and Perrin and Leblond (1993) identified these conditions, but at the time, physical evidence of compaction bands had not yet been discovered.

3 CONSTITUTIVE MODELS

Rudnicki and Rice (1975) suggested that formation of a planar band of localized strain in an inelastically deforming material could be viewed as a bifurcation from homogeneous deformation, due to an instability in the constitutive framework. The conditions of kinematic compatibility and stress equilibrium were combined with the constitutive relation, to determine that a band, with band normal components n_i, is possible when the condition det $|n_i\ L_{ijkl}\ n_l| = 0$ is satisfied. The modulus tensor, L_{ijkl}, defined by $d\sigma_{ij} = L_{ijkl}\ d\varepsilon_{kl}$, depends on details of the constitutive formulation, and thus the localization conditions are also influenced by the choice of constitutive relation. This work examines results from three existing constitutive models and a proposed new model for high porosity sandstone.

Wong and colleagues (Menéndez et al., 1996; Wu et al., 2000; Wong et al., 2001; Klein et al. 2001) examined the behavior of high porosity sandstones (Bentheim, Berea and Darley Dale, porosities of 23%, 21% and 13%, respectively). At lower confining pressures (path ASCa, Fig. 1a), in the brittle regime, microstructural observations found axial intragranular cracking and shear-induced debonding, leading to shear band formation. At high confining pressures (path ASCc, Fig. 1a) grain crushing and pore collapse occurred, and uniform compaction (cataclastic flow) with no evidence of strain localization was observed. At intermediate confining pressures (transitional regime, path ASCb, Fig. 1a), where compaction bands and/or shear bands occurred, both damage processes, axial microcracking and grain crushing with pore collapse, were active.

Issen (2002) suggested a two yield surface constitutive model (see Fig. 1a), to macroscopically represent the two damage processes active in the transitional regime. This model was derived using classical plasticity methods (for details, see Issen, 2002). Expressions for the shear yield surface and yield surface cap are: $F_1 = \tau - f_1\left(\sigma, \gamma^p\right) = 0$ and $F_2 = \sigma - f_2\left(\tau, \varepsilon^p\right) = 0$, respectively. The mean stress is $\sigma = -(1/3)\sigma_{kk}$ (positive in compression) and $\tau = \sqrt{(1/2)s_{ij}s_{ij}}$ is the second invariant of deviatoric stress, where the deviatoric stress is $s_{ij} = \sigma_{ij} - (1/3)\sigma_{kk}\delta_{ij}$, and δ_{ij} (= 1 if i = j, and = 0, if $i \neq j$) is the Kronecker delta, with repeated subscripts implying summation. The accumulated inelastic shear strain, γ^p, tracks inelastic deformation history for the first surface, while accumulated volume strain, ε^p, is used on the cap. The inelastic shear strain increment is

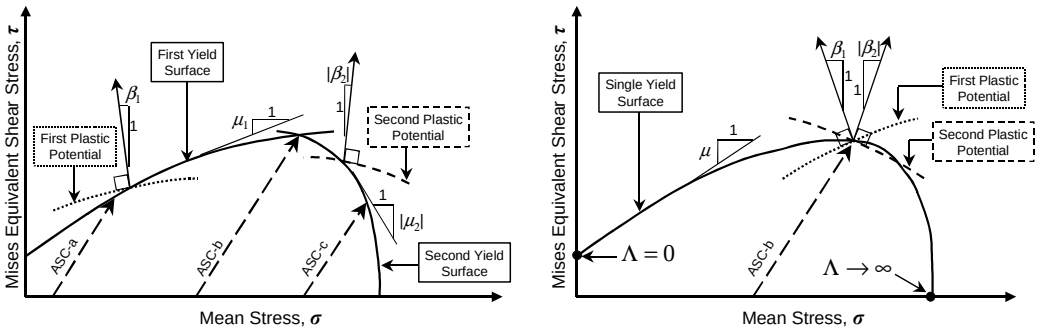

Figure 1: a) Two yield surface – two plastic potential model showing three axisymmetric (ASC) loading paths. b) Single yield surface – two plastic potential model.

defined as $d\gamma^p = \sqrt{2de_{ij}^p de_{ij}^p}$, where $de_{ij}^P = d\varepsilon_{ij}^P - (1/3)d\varepsilon_{kk}^P \delta_{ij}$ is the inelastic deviatoric strain, while the inelastic volume strain increment is $d\varepsilon^p = -d\varepsilon_{kk}^p$ (negative in compression). Non-associated flow was assumed, using the following expressions for the plastic potentials: $\Gamma_1 = \tau - g_1(\sigma, \gamma^p) = 0$ and $\Gamma_2 = \sigma - g_2(\tau, \varepsilon^p) = 0$. The slope of a yield surface is given by $\mu_i = -(\partial F_i / \partial \sigma)/(\partial F_i / \partial \tau)$, ($i$ = 1,2), where $\mu_1 > 0$, and $\mu_2 < 0$ (see Fig. 1a). Similarly, the slope of a plastic potential is $\beta_i = -(\partial \Gamma_i / \partial \sigma)/(\partial \Gamma_i / \partial \tau)$, also know as the dilation coefficient, where $\beta_1 > 0$ for dilatation and $\beta_2 < 0$ for volume compaction (see Fig. 1a).

Notice that, if the loading path clearly intersects only the first yield surface (path ASCa, Fig. 1a), then a single yield surface model, such as that used by Rudnicki and Rice (1975), and derived by Holcomb and Rudnicki (2001) using expressions F_1 and Γ_1, is applicable. Similarly, if the loading path intersects only the cap (path ASCc, Fig. 1a), a "cap" single yield surface model can be derived using expressions F_2 and Γ_2 (see Issen, 2002; Rudnicki, 2004). The expressions for the inelastic strain increments for these models are:

$$\left(d\varepsilon_{ij}^p\right)_1 = \frac{1}{h}\left(\frac{s_{ij}}{2\tau} + \beta_1 \frac{1}{3}\delta_{ij}\right)\left(\frac{s_{kl}}{2\tau} + \mu_1 \frac{1}{3}\delta_{kl}\right) d\sigma_{kl}\,, \tag{1}$$

$$\left(d\varepsilon_{ij}^p\right)_2 = \frac{1}{k\beta_2\mu_2}\left(\frac{s_{ij}}{2\tau} + \beta_2 \frac{1}{3}\delta_{ij}\right)\left(\frac{s_{kl}}{2\tau} + \mu_2 \frac{1}{3}\delta_{kl}\right) d\sigma_{kl}\,, \tag{2}$$

where the hardening moduli are h, the slope of the shear stress – inelastic shear strain curve at constant mean stress and k, the slope of the mean stress – inelastic volume strain curve at constant mean stress. For the two yield surface model, the increment of inelastic strain is determined by adding equations (1) and (2) (see Issen, 2002).

While the two yield surface model seems well suited to represent the two observed damage processes, the determination of two separate yield surfaces from experimental data can be difficult. Additionally, the model is strictly applicable only at the point where the two yield surfaces intersect, while the transitional regime occurs in a region of stress states near the intersection. Finally, it is still unclear whether the two yield surfaces intersect at a vertex, or if they meet smoothly, in which case, a single yield surface expression may be adequate. Therefore, this work proposes an alternate model, which employs a single yield surface, F_2, but retains the two plastic potentials, Γ_1 and Γ_2, representing the two damage processes observed in the transitional regime.

Using classical plasticity methods, the inelastic strain is determined from the flow rule:

$$d\varepsilon_{ij}^p = d\lambda_1 \frac{\partial \Gamma_1}{\partial \sigma_{ij}} + d\lambda_2 \frac{\partial \Gamma_2}{\partial \sigma_{ij}}\,. \tag{3}$$

It is necessary to define a damage characterization parameter, $\Lambda = d\lambda_2 / d\lambda_1$, which is the ratio of the magnitudes of the inelastic strain increments due to the two plastic potentials. Where the yield surface intersects the shear stress axis, $\Lambda = 0$, since $d\lambda_2 = 0$, because only dilatant microcracking is assumed to occur (see Fig. 1b). Moving along the yield surface toward the mean stress axis, Λ increases as some grain crushing begins, and axial microcracking becomes less prevalent. At the intersection with the mean stress axis, $\Lambda \to \infty$, because $d\lambda_1 = 0$, since only grain crushing with pore collapse is assumed to occur. Applying the consistency condition, $dF_2 = 0$, enables

determination of the expression for the inelastic strain for this constitutive model, which is found to be the identical to equation (2) for the single yield surface cap model, except that μ replaces μ_2, and β_2 is replaced by a combined dilation coefficient, $\beta = (\beta_1 + \Lambda\beta_2)/(1+\Lambda)$. Note that when $\Lambda = 0$, $\beta = \beta_1$ is recovered, while if $\Lambda \to \infty$, then $\beta = \beta_2$ is recovered.

4 LOCALIZATION CONDITIONS

Employing the localization theory of Rudnicki and Rice (1975), Issen and Rudnicki (2000, 2001) determined the band orientation predictions for a single yield surface model, using constitutive relation (1). For axisymmetric compression, shear bands are predicted when:

$$-\sqrt{3} \le \beta_\alpha + \mu_\alpha \le \sqrt{3}\left(\frac{2-\nu}{1+\nu}\right), \tag{4}$$

where $\alpha = 1$. Compaction bands are predicted when $\beta_1 + \mu_1 \le -\sqrt{3}$. The critical value of the hardening modulus at the inception of localization is given by $h_{cr} = \eta_1$, where

$$\eta_\alpha = -\frac{4G(1+\nu)}{9(1-\nu)}\left[\frac{27n_\ell^4}{8(1+\nu)} - \frac{3\sqrt{3}}{4}\left(\beta_\alpha + \mu_\alpha + \sqrt{3}\right)n_\ell^2 + \left(\beta_\alpha + \frac{\sqrt{3}}{2}\right)\left(\mu_\alpha + \frac{\sqrt{3}}{2}\right)\right], \tag{5}$$

and where G and ν are the elastic shear modulus and Poisson's ratio, and n_ℓ is the lateral component of the band normal (= 0 for compaction bands, = 1 for dilation bands). These results are shown graphically in Fig. 2a. Notice that the data reported by Olsson (1999) and Wong et al. (2001) do not satisfy the compaction band condition, even though compaction bands, as well as the predicted shear bands, were observed. If the single yield surface cap model, (2), is used, Issen (2002) and Rudnicki (2004), determined that the critical hardening modulus is $k_{cr} = \eta_2 / \beta_2\mu_2$, where η_2 is given by (5), with $\alpha = 2$. If β_2 and μ_2 are both negative (as is commonly assumed), then the shear band condition is again given by (4), and the compaction band condition is still

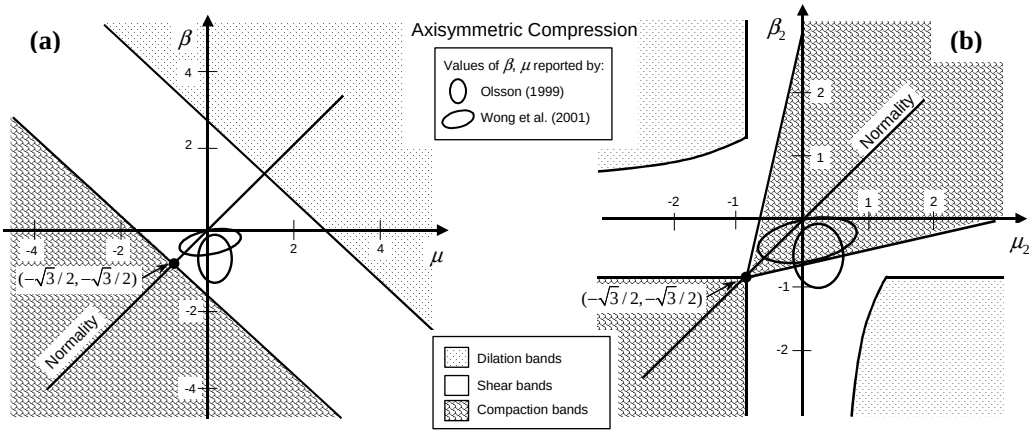

Figure 2: Predicted band orientations for a) single yield surface model and b) two yield surface model, for axisymmetric compression

$\beta_2 + \mu_2 \le -\sqrt{3}$. The band orientation predictions in the third quadrant of Fig. 2a are applicable.

For the proposed single yield surface – two plastic potential model, we find that the critical hardening modulus expression is the same as the single yield surface cap model, except that the cap slope, μ_2 is replaced by the single yield surface slope, μ, and β_2 is replaced by the combined dilation coefficient, β. Therefore, $k_{cr} = \eta / \beta\mu$, and the subscript α is dropped. Similar to the single yield surface cap model, if β and μ are assumed to be negative, corresponding to overall compactive deformation, then the compaction band condition remains $\beta + \mu \le -\sqrt{3}$, and the band orientation predictions in the third quadrant of Fig. 2a are still applicable. Therefore, although the flexibility of an additional plastic potential has been added to the single yield surface model, the localization conditions have not changed when the overall material behavior is compactive. Thus, the values of β and μ reported by Olsson (1999) and Wong et al. (2001) still do not satisfy the compaction band condition.

For the two yield surface – two plastic potential model, the critical hardening modulus, as determined by Challa and Issen (2004) is $h_{cr} = \left(k\beta_2\mu_2\eta_1 + C\right) / \left(k\beta_2\mu_2 - \eta_2\right)$, where $C = -\left(1+\nu\right) / \left[3\left(1-\nu\right)\right] G^2 \left(\beta_1 - \beta_2\right)\left(\mu_1 - \mu_2\right) n_\ell^4$. Since compaction band formation is typically observed to occur at or near the stress peak in the mean stress – volume strain curve, $k \approx 0$ is a reasonable assumption. Even with this simplification, the localization conditions cannot be meaningfully expressed in a single equation, similar to (4). However, the band orientation predictions can be depicted graphically, as shown in Fig. 2b, in terms of β_2 and μ_2 (Challa and Issen, 2004, found that the band orientation predictions do not depend on β_1 and μ_1 when $k = 0$). Using this model, both the observed compaction bands and shear bands are predicted for the values of β and μ reported by Olsson (1999) and Wong et al. (2001). Note that experimentalists report single values of β and μ, while this model requires β_1, μ_1, β_2 andμ_2. However, it can be shown that $\beta_2 < \beta < \beta_1$ and $\mu_2 < \mu < \mu_1$ are typically true. Therefore, values for β_2 andμ_2 will likely fall to the left and below the reported values of β and μ, such that the observed compaction bands and dilation bands will likely still be predicted.

5 CONCLUSIONS

This work examined the influence of four different constitutive models on strain localization conditions for high porosity rock. The models were derived via classical plasticity methods, assuming non-associated flow, and used either one or two yield surfaces, and one or two plastic potentials. Two different single yield surface – single plastic potential models were considered: the "shear" yield surface model of Rudnicki and Rice (1975), originally developed for a dilatant material, and the "cap" model developed by Issen (2002) and Rudnicki (2004), for compacting materials. The two yield surface – two plastic potential model of Issen (2002), which seeks to represent the two microstructurally observed damage processes of dilatant microcracking and compactive grain crushing with pore collapse, was also examined. Finally, a new single yield surface – two plastic potential model was proposed, which represents the two damage processes with two plastic potentials, but employs a simplified single yield surface. In this model, a damage characterization parameter, Λ, is used to represent the ratio of the magnitudes of the two inelastic strains due to the two damage processes. This parameter can be utilized to establish a region where both process are active, corresponding to the observed brittle – ductile transitional regime. This circumvents an inconvenient restriction in the two yield surface model, i.e., the model is strictly applicable only at the point of intersection of the two yield surfaces.

Using the Rudnicki and Rice (1975) localization theory, strain localization conditions were determined for the four constitutive models. For overall compactive behavior (i.e., the dilation

coefficient, β, and yield surface slope, μ, are both negative), all three of the single yield surface models, including the proposed new model, lead to the same band orientation predictions, and compaction bands are possible only when $\beta + \mu \leq -\sqrt{3}$. However, using the data reported by Olsson (1999) and Wong et al. (2001), only shear bands, and not the observed compaction bands and shear bands are predicted. Therefore, the additional flexibility provided by adding a second plastic potential to a single yield surface model does not alter the constitutive framework enough to affect the fundamental aspects of the localization conditions. However, the addition of a second yield surface with the second plastic potential (Issen, 2002; Challa and Issen, 2004), significantly alters both the constitutive framework and the localization conditions, such that this model predicts both observed compaction bands and shear bands.

ACKNOWLEDGMENTS

Financial support provided by the National Science Foundation, Geosciences Directorate, Earth Sciences Division, grant EAR-0310085 to Clarkson University, in collaboration with T.-f. Wong, SUNY Stony Brook.

REFERENCES

Challa V and Issen KA, 2004, Conditions for Compaction Band formation in porous rock using a two yield surface model, *J Engg Mech*, **130**(9), in press.

Holcomb, D. J. and Rudnicki, J. W. 2001. Inelastic Constitutive Properties and Shear Localization in Tennessee Marble. *Int J Numerical Analytical Methods Geomechics*, **25**, 109-129.

Issen KA and Rudnicki JW, 2000, Conditions for compaction bands in porous rock. *J Geophys Res*, **105**(B9), 21529-21536.

Issen KA and Rudnicki JW, 2001, Theory of compaction bands in porous rock. *Phys Chem Earth (A)*, **26**(1-2), 95-100.

Issen KA, 2002, The influence of constitutive models on localization conditions for porous rock. *Engg Frac Mech*, **69**, 1891-1906.

Klein, E., Baud, P., Reuschlé, T., and Wong, T.-f. (2001). "Mechanical behavior and failure mode of Bentheim sandstone under triaxial compression," *Phys. Chem. Earth.* (A), 26(1-2), 21-25.

Menéndez B, Zhu W and Wong T-f, 1996, Micro mechanics of brittle faulting and cataclastic flow in Berea sandstone. *J Struct Geol*, **18** (1), 1-16.

Mollema PN and Antonellini MA, 1996, Compaction bands: a structural analog for anti-mode I cracks in Aeolian sandstone. *Techtonophysics*, **267**, 209-228.

Olsson WA, 1999, Theoretical and experimental investigation of compaction bands. *J Geophy Res*, **104**, 7219-7228.

Ottosen, N. S., and Runesson, *K*. (1991). "Properties of discontinuous bifurcation solutions in elasto-plasticity," *Int. J. Solids. Struct.*, 27 (4), 401-421.

Perrin, *G*., and Leblond, L. B. (1993). "Rudnicki and Rice's analysis of strain localization revisited," *J Appl Mech*, 60, 842-846.

Rudnicki JW and Rice JR, 1975, Conditions for the localization of deformation in pressure-sensitive dilatant materials. *J Mech Phys Solids*, **23**, 371-394.

Rudnicki, J.W. 2004. Shear and compaction band formation on an elliptic yield cap. *J Geophys Res*, **109**(B3), B03402.

Wong T-f, Baud P and Klein E, 2001, Localized failure modes in compactant porous rock. *Geophys Res Lett*, **28**(13), 2521-2524.

Wu XY, Baud P and Wong T-f, 2000, Micromechanics of compressive failure and spatial evolution of anisotropic damage in Darley Dale sandstone. *Int J Rock Mech Mining Sci*, **37**, 143-160.